IV.C.3 Multiply Surface-Functionalized Nanoporous Carbon for Vehicular Hydrogen Storage

P. Pfeifer (Primary Contact), C. Wexler, P. Yu, G. Suppes, F. Hawthorne, S. Jalisatgi, M. Lee, D. Robertson
University of Missouri
223 Physics Building
Columbia, MO 65211
Phone: (573) 882-2335
E-mail: pfeiferp@missouri.edu

DOE Managers
HQ: Ned Stetson
Phone: (202) 586-9995
E-mail: Ned.Stetson@ee.doe.gov
GO: Jesse Adams
Phone: (720) 356-1421
E-mail: Jesse.Adams@go.doe.gov

Contract Number: DE-FG36-08GO18142

Subcontractor:
Midwest Research Institute, Kansas City, MO

Project Start Date: September 1, 2008
Project End Date: January 31, 2013

Fiscal Year (FY) 2011 Objectives

- Fabricate high-surface-area, multiply surface-functionalized carbon ("substituted materials") for reversible hydrogen storage with superior storage capacity (strong physisorption).
- Characterize materials and storage performance. Evaluate efficacy of surface functionalization, experimentally and computationally, for fabrication of materials with deep potential wells for hydrogen sorption (high binding energies).
- Optimize gravimetric and volumetric storage capacity by optimizing pore architecture and surface composition ("engineered nanospaces").

Technical Barriers

This project addresses the following technical barriers from the Hydrogen Storage section of the Fuel Cell Technologies Program Multi-Year Research, Development and Demonstration Plan:

(A) System Weight and Volume

(B) System Cost

(E) Charging/Discharging Rates

(J) Thermal Management

(P) Lack of Understanding of Hydrogen Physisorption and Chemisorption

Technical Targets

This project aims at the development of surface-engineered carbons, made from corncob or other low-cost raw materials, which simultaneously host high surface areas, created in a multi-step process, and a large fraction of surface sites with high binding energies for hydrogen, created by surface functionalization with boron, iron, and lithium. Targets are surface areas in excess of 4,500 m^2/g, average binding energies in excess of 12 kJ/mol, and porosities below 0.8, toward the design of materials that meet the following 2015 DOE hydrogen storage targets:

- Gravimetric storage capacity: 0.055 kg H_2/kg system
- Volumetric storage capacity: 0.040 kg H_2/liter system

FY 2011 Accomplishments

- Manufactured boron-substituted carbon by deposition and thermolysis of $B_{10}H_{14}$ on high-surface-area activated carbon, with B:C = 7-10 wt%, without compromising high surface areas (≥2,100 m^2/g). Developed plans for automated apparatus.
- Maintained an oxygen- and water-free environment for the manipulation, characterization, and analysis of boron-substituted carbon, which was fundamental for the observation of enhanced hydrogen sorption characteristics.
- Observed an increase of 30% in areal excess adsorption (excess adsorption per surface area) of hydrogen, at $T = 303$ K and $P = 200$ bar, on boron-substituted carbon (B:C = 8.6 wt%) compared to its boron-free precursor. The increase in excess adsorption at high temperature and pressure demonstrates an increase in average binding energy due to boron substitution.
- Optimized pore structure of undoped carbons by varying the KOH:C ratio and temperature during activation. High KOH:C and T lead to larger surface area, pore volume, and porosity, but a reduced fraction of narrow pores. Optimal conditions for hydrogen storage are observed for activation with a 3.5 KOH:C ratio at 800°C, which represents the best balance between increasing the pore volume and loss of high-binding-energy sites in narrow pores.
- At low KOH:C and T, the pore structure is consistent with large graphene sheets closely stacked, whereas for more aggressive activation conditions the pores are formed by small graphene sheets loosely stacked (surface areas larger than that of graphene, 2,600 m^2/g).

- Observed that carbon monoliths formed by activated carbon and polyvinylidine chloride (PVDC) binder outperforms powder samples at room temperature, consistent with findings that pyrolyzed PVDC is an attractive material for hydrogen storage (sample HS;0B) [1].
- Developed and applied a consistent method for the determination of isosteric heat of adsorption from the Clausius-Clapeyron equation. Validated by microcalorimetry measurements. The thermodynamic requirement that the isosteric heat cannot increase with increasing pressure and coverage gives a lower bound for the adsorbed film thickness (or volume).
- Established, via Fourier-transform infrared spectroscopy (FTIR), the presence of B-C bonds in boron-doped carbons (1,022 cm^{-1} line).

Introduction

High-surface-area carbons from corncob, as developed by our team, show considerable promise for reversible onboard storage of hydrogen at high gravimetric and volumetric storage capacity. An earlier carbon exhibited a gravimetric storage capacity of 0.11 kg H_2/kg carbon at 80 K and 50 bar. This project is a systematic effort to achieve comparable results at 300 K, by increasing surface areas from currently ~3,000 m^2/g to ~6,000 m^2/g, and substituting carbon with boron and other elements that increase the binding energy for hydrogen (electron donation from H_2 to electron-deficient B, and other charge-transfer mechanisms). Earlier high surface areas and high binding energies were hosted by sub-nm pores ("nanopores") in narrowly spaced "stacks of graphene sheets." New high-surface-area, boron-substituted materials are manufactured by thermolysis of volatile boron carriers in pores of stacks of graphene sheets. New surface area, created by fission tracks from boron neutron capture, in stacks of boron-substituted graphene sheets, or created in the form of stacks of small graphene sheets with large ratio of edge sites to in-plane sites, may add as much as another 3,000 m^2/g.

Approach

The approach is an integrated fabrication, characterization, and computational effort. Structural characterization includes determination of surface areas, pore-size distributions, and pore shapes. Storage characterization includes measurements of hydrogen sorption isotherms and isosteric heats. Computational work includes adsorption potentials and simulations of adsorbed films for thermodynamic analysis of experimental isotherms. Comparison of computed and experimental isotherms validates theoretical adsorption potentials and experimental structural data.

Results

Observation of Enhanced Hydrogen Sorption on Boron-Doped Samples

Upgrades to the laboratory during the current year allowed us to process for the first time all boron-doped samples in oxygen- and water-free conditions. Activated carbon samples were degassed and coated with a monolayer or less of decaborane, $B_{10}H_{14}$, by liquid/vapor deposition (Figure 1), followed by pyrolysis and high-temperature annealing. This process creates the necessary boron substitution (FTIR indicates B-C bonds consistent with B-substitution in the C matrix). Table 1 shows selected samples manufactured and their characteristics. Hydrogen sorption isotherms for selected samples are shown in Figure 2. For B:C = 8.6 wt%, the areal excess adsorption at 303 K and 200 bar is 30% higher than on undoped material. The fact that the increase is observed at high temperature and pressure demonstrates an increase in the average binding energy, not highest binding energy. This is consistent with that sample 3K-H60 (I,A) was doped by Method I (liquid deposition), which deposits significant amounts of boron only in large pores. An increase in H_2 sorption is not observed at 90 K because unblocked pores in undoped material support H_2 multilayers, not available in the doped material. O_2-free conditions were crucial for increased adsorption on B-doped samples (prior to the laboratory upgrade, no increase in H_2 sorption was observed in B-doped samples that had been exposed to air).

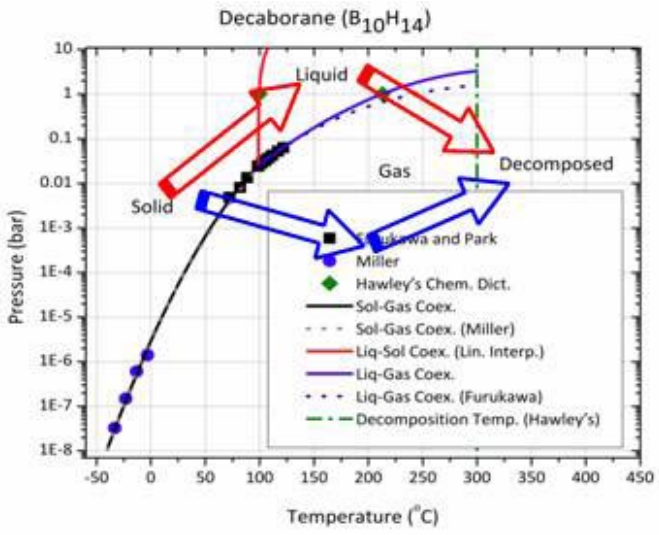

FIGURE 1. Schematic representation of deposition methods I (red, "liquid phase") and III (blue, "vapor phase"). Higher deposition rates are possible with Method I, but since the process involves liquid decaborane, pore blocking may occur, as indicated by the reduction in Brunauer-Emmett-Teller (BET) surface area (Table 1).

TABLE 1. Sample characteristics of boron-doped carbons. B:C concentration was determined by prompt gamma neutron activation analysis.

Sample	Precursor	B:C (wt%)	Σ_{N2} (m^2/g)	Φ_{N2}	Notes
3K 3/3/10-B	Self	0.0	2,700	0.77	
3K-H30 (I,A)	3K 3/3/10-B	8.4	2,300	0.75	B-H decomp., 600°C
3K-H31 (III,A)	3K 3/3/10-B	10.0	2,000	0.73	B-H decomp., 600°C
3K 3/3/10-B degassed @ 600°C	Self	0.0	2,600	0.76	
3K-H60 (I,A)	3K 3/3/10-B degassed @ 600°C	8.6	2,100	0.73	B-H decomp., 600°C
3K-H60 (I,B)	3K 3/3/10-B degassed @ 600°C	6.7	2,100	0.72	B-H decomp., 1,000°C

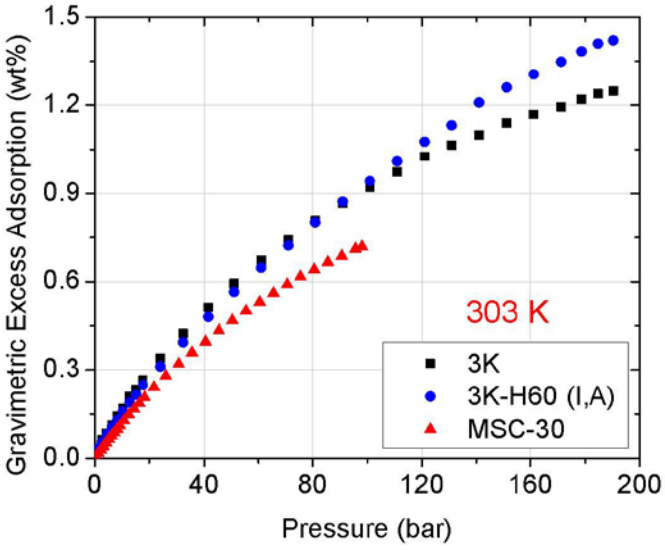

FIGURE 2. Hydrogen sorption on boron-doped sample 3K-H60 (I,A), its boron-free precursor (3K 3/3/10-B), and reference sample MSC-30 (Maxsorb, Kansai Coke and Chemicals, Ltd). Experimental results are from 4-9 adsorption/desorption isotherms and are highly reproducible. Areal excess adsorption on 3K-H60 (not shown) is 30% higher than on 3K.

Optimization of Pore Geometry

Efforts to optimize the pore geometries of carbon precursors for hydrogen sorption were undertaken as follows. Ground corncob is soaked with phosphoric acid and charred at 480°C under nitrogen. The carbon is then activated by KOH in an oven, resulting in oxidation of some carbon by oxygen, and penetration of metallic potassium into the graphitic lattice. The intercalated potassium separates the graphene sheets/flakes and results in the formation of a highly porous material upon removal of the alkali. The resulting structure can be controlled by the weight ratio of KOH:C and activation temperature. Table 2 shows sample characteristics and H_2 sorption for various samples activated under different KOH:C ratios and temperatures (Figures 3-4). High KOH:C and temperature lead to larger surface area, pore volume, and porosity, but at the cost of a reduction of fraction of narrow pores. Optimal conditions for hydrogen storage are observed for activation with a KOH:C of 3.5 ratio at 800°C, which represents the best balance between a large pore volume and a small loss of high-binding-energy sites in narrow pores. At low KOH:C and temperature, the pore structure is consistent with large graphene sheets closely stacked, whereas for more aggressive

TABLE 2. Sample characteristics of carbon precursors. Names indicate KOH:C weight ratio and temperature during activation (e.g., 3K 900°C was activated with KOH:C = 3 at 900°C). Specific surface areas, Σ_{N2}, from BET analysis of N_2 adsorption isotherms at 77 K and relative pressures 0.01-0.03, are rounded to nearest hundred. Porosities, Φ_{N2}, were determined from N_2 adsorption at 77 K at relative pressure 0.995. Values for gravimetric excess adsorption are presented for P = 100 bar at 80 K, 194 K, and 303 K. Best performances in each column are highlighted in bold face.

Sample	Σ_{N2} (m^2/g)	Φ_{N2}	Grav. Exc. Ads. 100 bar, 303 K (wt%)	Grav. Exc. Ads. 100 bar, 194 K (wt%)	Grav. Exc. Ads. 100 bar, 80 K (wt%)
2.5K 800°C	1,900	0.69	0.53	1.62	N/A
3K 700°C	2,200	0.65	0.67	2.01	N/A
3K 800°C	2,200	0.78	0.74	2.12	4.47
3K 900°C	2,500	0.78	**0.82**	**2.28**	4.68
3K 1000°C	2,000	0.78	0.60	1.80	4.05
3.5K 700°C	2,000	0.70	0.63	1.85	4.42
3.5K 800°C	2,500	0.75	**0.84**	**2.18**	**5.15**
3.5K 900°C	2,500	0.78	0.70	2.14	**5.18**
4K 800°C	2,600	0.81	0.56	N/A	5.02
5K 790°C	2,500	0.79	0.65	N/A	4.03

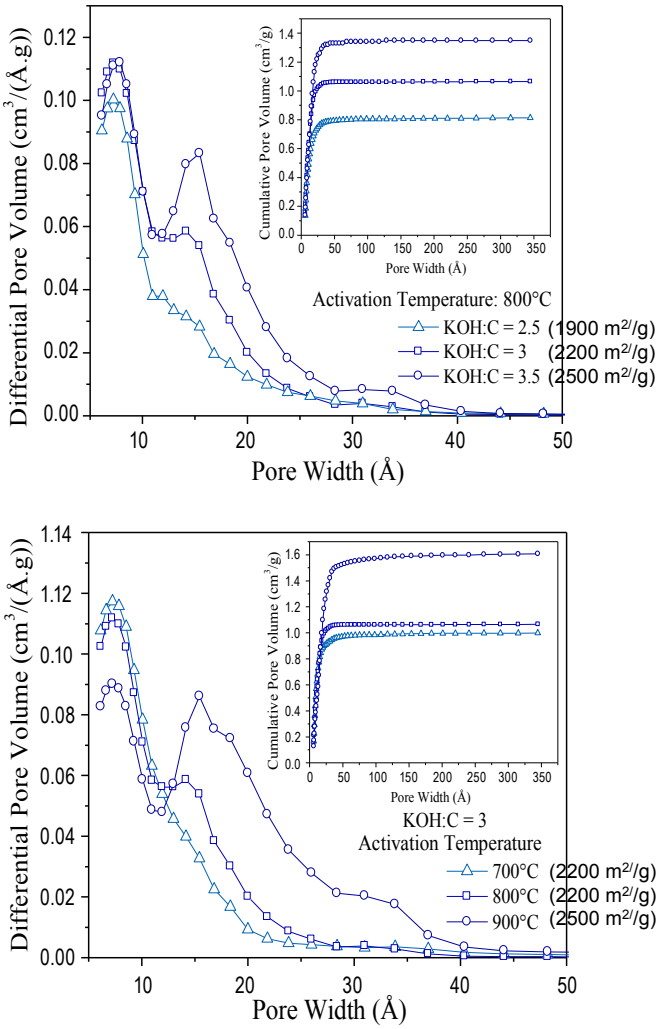

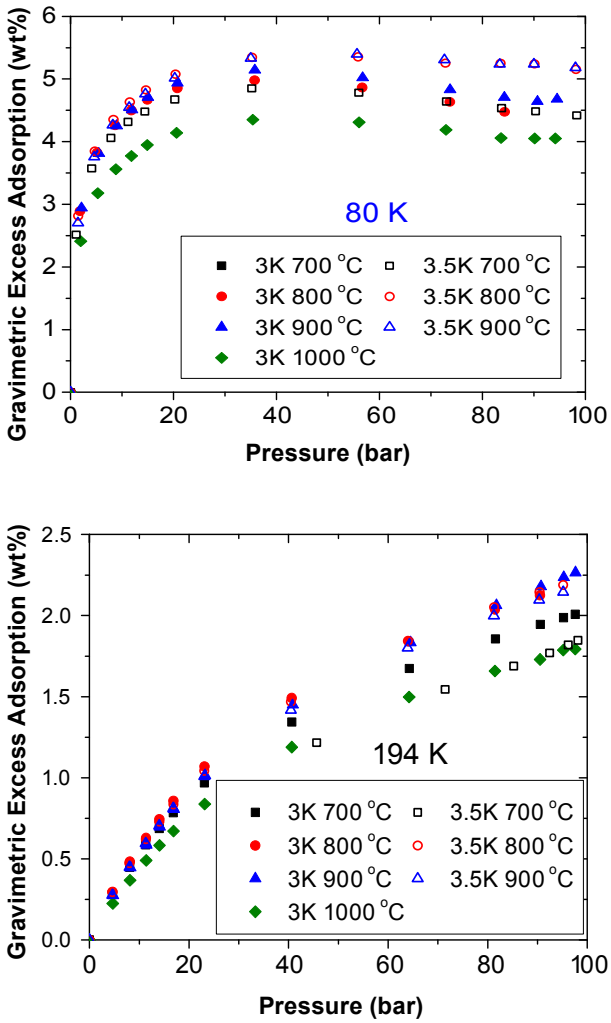

FIGURE 3. Differential and cumulative pore-size distribution from nitrogen adsorption for various activated carbons. Top: variation of KOH:C ratio at constant activation temperature. Bottom: variation of activation temperature at constant KOH:C ratio.

FIGURE 4. Gravimetric excess adsorption of H_2 on carbons produced with different KOH:C ratios and activation temperatures. Results are shown at T = 80 K, 194 K (dry-ice temperature), and 303 K.

activation conditions the pores are formed by small graphene sheets loosely stacked (edge sites generate surface areas larger than that of graphene, 2,600 m^2/g).

Comparison of Powders and Monoliths (Briquettes)

One method to enhance the volumetric storage capacity is to increase the density the activated carbon. We have investigated this densification by "briquetting," i.e., the production of monoliths. Powdered activated carbon was pressed into briquettes at 1,000 bar using PVDC as a binder (PVDC:carbon = 25-30 vol%), followed by pyrolysis of PVDC. The mass of a typical briquette was 70-100 g. Hydrogen sorption on briquettes was measured volumetrically for entire briquettes on a custom instrument with a 0.5-liter sample chamber ("Hydrogen Test Fixture,"

TABLE 3. Comparison of powdered activated carbon and three carbon monoliths (briquettes). All hydrogen adsorption data are at room temperature, 297 K, and 100 bar. Gravimetric and volumetric storage capacities were calculated based on intragranular porosity (from N_2 adsorption at 77 K) for powders, and on intergranular porosity (from bulk density) for briquettes, respectively [2]. All hydrogen measurements on briquettes were performed on the HTF. Best performances are highlighted in bold face.

Sample	Σ_{N2} (m^2/g)	Intragranular (intergranular) Density (g/cm^3)	Φ_{N2}	Grav. Exc. Ads. (wt%)	Grav. Storage Cap. (wt%)	Vol. Storage Cap. (g/L)
2.5K powder	1,900	0.62	0.69	0.53	1.3	8.2
3K powder	2,600	0.44	0.78	**0.93**	2.2	9.6
4K powder	2,600	0.38	0.81	0.56	2.1	7.8
MSC-30	2,600	0.42	0.79	0.72	2.3	8.8
2.5K Briquette (30% binder)	2,000	0.74 (0.70)	0.63 (0.65)	0.67	1.4	**9.7**
3K Briquette (25% binder)	1,900	0.56 (0.47)	0.72 (0.77)	0.75	2.0	9.5
4K Briquette (25% binder)	2,100	0.53 (0.37)	0.74 (0.81)	0.86	**2.6**	9.5

HTF). Measurements on the HTF were validated on the Hiden HTP-1 instrument. Table 3 shows a comparison of four activated carbon powders and three briquettes. We observe that: (a) briquetting raises the density of samples by 20-40%, relative to the powder; (b) carbon made from PVDC exhibits superior hydrogen uptake at room temperature (HS;0B; very high areal excess adsorption [1]); (c) briquettes outperform most powder samples in terms of volumetric storage capacity because low porosity gives high volumetric storage capacity; (d) all briquettes outperform MSC-30 at room temperature in terms of volumetric storage capacity and areal excess adsorption. 4K briquette outperforms MSC-30 also in terms of gravimetric storage capacity; (e) entire briquettes, measured on the HTF, lead to robust averages over possible sample inhomogeneities. A 10-liter tank, recently completed [3], will permit studies of flow rates, thermal management, and operation at dry-ice temperature (194 K).

Observation of B-C Bonds by Fourier-Transform Infrared Spectroscopy

FTIR spectroscopy was used in transmission mode to identify the presence of boron-carbon bonds in boron-doped activated carbon. An infrared spectrum represents a fingerprint of a sample with absorption peaks, which correspond to vibrational frequencies of structural units making up the material. The samples were prepared using KBr pellets with a sample/KBr ratio of 0.033 wt%. Each FTIR spectrum was collected as an average of 32 interferometric scans with a spectral resolution of 1 cm^{-1}. An aperture was used to limit the sampling size and select the sampling area (>10 µm). Figure 5 shows the microscopic FTIR spectra for boron-free and boron-containing carbons. The FTIR spectrum of boron-free sample 3K shows only carbon-related bands, including the C-OH stretch mode at 3,429 cm^{-1}, C-OH bend mode at 1,630 cm^{-1}, C=C double-bond stretch mode at 1,430 cm^{-1}, and C-O bond stretch mode at 1,050 cm^{-1}. B-C bonds in boron-doped samples, 3K-H30 (not shown) and 3K-H31 (Figure 5), were identified by comparing spectra with the spectrum of an activated boron carbide (not shown), a reference with the 1,022 cm^{-1} band characteristic of B-C bonds. The band at 1,022 cm^{-1} demonstrates the successful creation of boron-carbon bonds. Samples 3K-H30 and 3K-31, in addition to exhibiting C-OH and C-O modes seen in boron-free sample 3K, also exhibit a B-OH stretch mode at 3,220 cm^{-1} and B-O stretch mode 1,327 cm^{-1}, consistent with the fact that the samples were not kept in an oxygen- and water-free environment for the FTIR experiment. To the best of our knowledge, this is the first time that the existence of B-C bonds in boron-doped carbons (liquid/vapor deposition of $B_{10}H_{14}$) has been observed and, hence, the successful incorporation of boron in the carbon matrix has been demonstrated.

Conclusions and Future Directions

- Observed enhanced hydrogen physisorption in boron-doped samples, enabled by equipment upgrades, with operations in an inert atmosphere.
- Optimized pore structure of samples by control of KOH:C ratio and temperature during activation.
- Performed comparison of powders and monoliths: increase in room-temperature performance of monoliths attributed to presence of pyrolized PVDC [1].
- Established B-C bonds by means of Fourier-transform infrared spectroscopy.
- Future work: (a) Continue production and characterization of B-doped samples, using $B_{10}H_{14}$ as boron carrier; investigate chemical pathways during the pyrolysis of $B_{10}H_{14}$ and annealing (mass spectroscopy of decomposition products) and effects on H_2 storage; optimize pathway of vapor/liquid deposition of $B_{10}H_{14}$; raise surface area of doped samples by removal of B via high-temperature reaction with H_2; optimize annealing. (b) Measure FTIR spectra of B-doped samples systematically; find number of B-C bonds per surface area. (c) Characterize B-doped materials produced from BCl_3 and compare with B-doping from

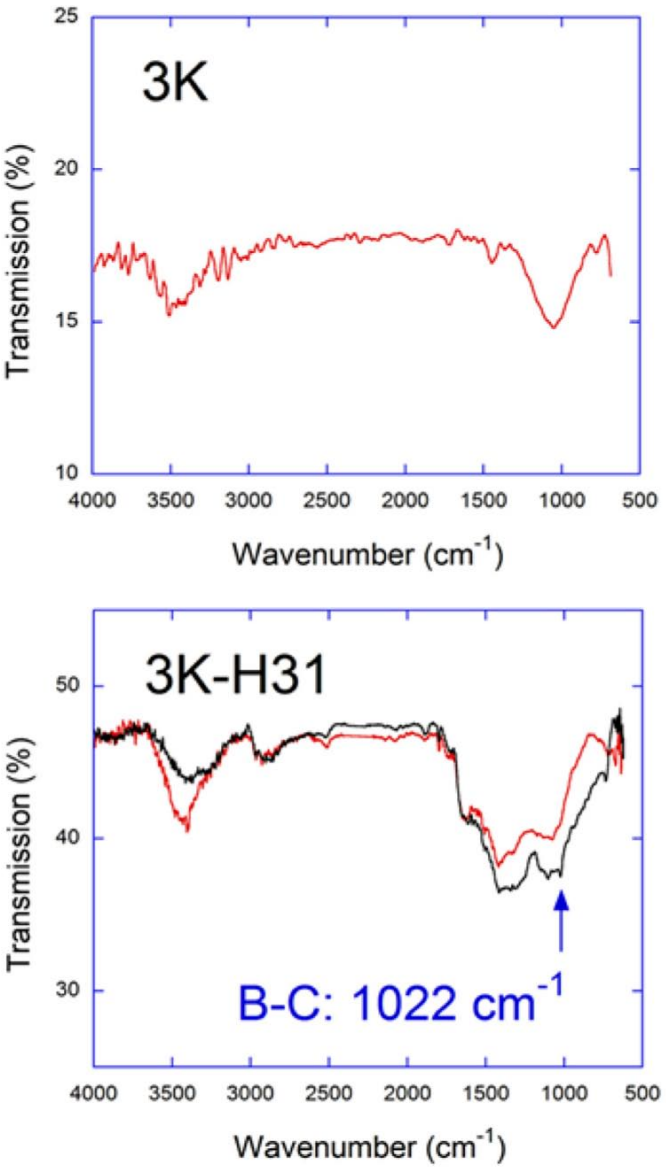

FIGURE 5. Microscopic FTIR spectra for samples 3K 3/3/10-B (boron-free) and 3K-H31 (III,A) (boron-doped). Each spectrum was obtained by limiting and selecting the sampling area through an aperture of an optical microscope (FTIR microscopy). The peak at 1,022 cm^{-1} is due to the B-C bond. The two spectra in 3K-H31 (III,A) correspond to different sampling locations.

$B_{10}H_{14}$. (d) Perform numerical simulations to investigate edge adsorption in finite pores, and compare results with experimental results on carbons activated at high KOH:C and high *T*. Determine pore structure and energetics from experimental H_2 isotherms. (e) Manufacture B-doped monoliths; test in 0.5-liter HTF and 10-liter tank; study flow rate and thermal management issues.

FY 2011 Publications/Presentations

1. R. Olsen, "Investigations of Novel Hydrogen Adsorption Phenomena." Ph.D. Dissertation, University of Missouri (2011).

2. C. Wexler, R. Olsen, P. Pfeifer, B. Kuctha, L. Firlej, Sz. Roszak, "Numerical Analysis of Hydrogen Storage in Carbon Nanopores." Int. J. Mod. Phys. B **24**, 5152-5162 (2010).

3. R.J. Olsen, L. Firlej, B. Kuchta, H. Taub, P. Pfeifer, and C. Wexler, "Sub-Nanometer Characterization of Activated Carbon by Inelastic Neutron Scattering." Carbon **49**, 1663-1671 (2011).

4. B. Kuchta, L. Firlej, S. Roszak, and P. Pfeifer, "A Review of Boron Enhanced Nanoporous Carbons for Hydrogen Adsorption: Numerical Perspective." Adsorption **16**, 413-21 (2010).

5. C. Wexler, P. Pfeifer, M. Kraus, M. Beckner, J. Romanos, D. Stalla, T. Rash, H. Taub, P. Yu, R. Olsen, and J. Ilavsky, "Characterization of Activated Carbon at the sub-nm Scale via Adsorption, TEM, FTIR, IINS and SAXS; and Application towards Optimization of H_2 Storage." *9th International Symposium on the Characterisation of Porous Solids (COPS 9)*, DECHEMA, Dresden, Germany, June 2011.

6. P. Pfeifer, C. Wexler, G. Suppes, F. Hawthorne, S. Jalisatgi, M. Lee, and D. Robertson, "Multiply Surface-Functionalized Nanoporous Carbon for Vehicular Hydrogen Storage." *2011 DOE Hydrogen Program Annual Merit Review*, Arlington, VA, May 9–13, 2011.

7. C. Wexler, "A Nanoporous Carbon 'Sponge' for Hydrogen Storage." Physics Colloquium, University of Buffalo, Buffalo, NY, April 2011.

8. Plus: 3 posters at various conferences and 7 contributed oral presentations at the APS March Meeting.

9. R. Olsen and C. Wexler, "Explaining the Hydrogen Adsorption of a Carbon Adsorbent Manufactured by the Pyrolosis of Saran." Physics Colloquium, University of Northern Iowa, Cedar Falls, IA, January 2011.

References

1. P. Pfeifer *et al.*, In: *DOE Hydrogen Program, FY 2010 Annual Progress Report*, ed. by S. Satyapal (U.S. Department of Energy, Washington, D.C., 2011), p. 474-480.

2. P. Pfeifer *et al.*, In: *DOE Hydrogen Program, FY 2009 Annual Progress Report*, ed. by S. Satyapal (U.S. Department of Energy, Washington, D.C., 2009), p. 646-651.

3. Work performed under a different project.